Available online at www.sciencedirect.com
SCIENCE DIRECT®
International Journal of Mass Spectrometry 229 (2003) 199–208
International Journal of Mass Spectrometry
www.elsevier.com/locate/ijms

Gas-phase non-identity S_N2 reactions at neutral nitrogen: a hybrid DFT study

Jing Yang [a], Yi Ren [a,*], Hua-jie Zhu [b,1], San-Yan Chu [c]

[a] *Faculty of Chemistry, Sichuan University, Chengdu 610064, PR China*
[b] *State Key Lab of Phytochemistry and Plant Resources in West China, CAS, Kunming 650200, PR China*
[c] *Department of Chemistry, National Tsing Hua University, Hsinchu 30013, Taiwan, ROC*

Received 15 May 2003; accepted 24 June 2003

Abstract

The gas-phase non-identity nucleophilic substitution reactions at saturated nitrogen $Y^- + NH_2X \rightarrow NH_2Y + X^-$ (Y, X = F, Cl, Br and I) were evaluated at the level of MPW1K/6-31+G(d, p). The enthalpies of reactions are exothermic only when the nucleophile is the lighter halide. Central barriers ($\Delta H^{\neq}_{YX}$) for reactions in the exothermic direction are slightly higher than the corresponding barriers at carbon. The lower overall barriers relative to the reactants (ΔH^{b}_{YX}) than the corresponding reactions at carbon suggest that S_N2 reactions at nitrogen may be more facile than at carbon. Both the central barriers ($\Delta H^{\neq}_{YX}$) and the overall barriers (ΔH^{b}_{YX}) correlate well with reaction exothermicity. Further interesting features of the non-identity reactions at nitrogen are the reasonable correlation between the central barriers ($\Delta H^{\neq}_{YX}$) with the composite geometrical looseness (%$L^{\neq}$), geometrical asymmetry (%$AS^{\neq}$), and charge asymmetry of the transition structures (Δq (X − Y)). The data for the central barriers and the overall barriers show good agreement with the prediction of the Marcus equation and its modification, respectively. Kinetic and thermodynamic investigations predict that the nucleophilicity of X^- in the S_N2 at nitrogen decreases in the order $F^- < Cl^- < Br^- < I^-$, the leaving-group ability increases in the order F > Cl > Br > I.

Keywords: S_N2 at neutral nitrogen; Hybrid DFT method; Reaction mechanism; Nucleophilicity

1. Introduction

The S_N2 nucleophilic displacement at saturated carbon in the gas phase is probably the most intensively studied of all chemical reactions [1–6]. In the last decade, S_N2 reactions at formal neutral nitrogen have become the focus of interesting attention because of their synthetic, biochemical and theoretical importance. Using double labeling experiments, Beak and Li [7] inferred the existence of a classical S_N2 transition state at a nitrogen substrate in the liquid phase. Theoretical studies of Bühl and Schaefer [8] support the existence of conventional backside S_N2 transition state structures in reactions $Y^- + NH_2X \rightarrow NH_2Y + X^-$ at the ab initio DZP+/SCF level of theory for Y, X = F, Cl, OH, CN, H. Glukhovtsev et al. [9] and Ren et al. [10] reported high-level calculation for the gas-phase identity S_N2 reactions $X^- + NR_2X \rightarrow NR_2X + X^-$ (R = H, Me, X = F, Cl, Br, I) using the G2 (+) theory, respectively. Gareyev et al. [11] studied the reactions of NH_2Cl with HO^-, RO^- (R = CH_3, CH_3CH_2, $CH_3CH_2CH_2$, $C_6H_5CH_2$, CF_3CH_2), F^-, HS^-, and Cl^- in the gas phase using the selected ion flow tube technique and found that nucleophilic substitution at nitrogen to form Cl^- were observed for all the nucleophiles and these S_N2 reactions were faster than the corresponding S_N2 reactions of methyl chloride. All of these study revealed some similarities and differences between anionic S_N2 reactions at nitrogen and carbon.

In the G2 (+) study on the non-identity S_N2 reactions of halide anions with methyl halides (see Eq. (1)), Glukhovtsev et al. [12] explored the role of reaction thermodynamics in governing barrier heights and thereby tested the applicability of Marcus theory [13–15] and the additivity postulate [14] for intrinsic energies.

$$Y^- + CH_3X \rightarrow CH_3Y + X^- \quad (Y, X = F, Cl, Br \text{ and } I) \tag{1}$$

* Corresponding author. Tel.: +86-28-85412800; fax: +86-28-85257397.
E-mail addresses: yiren57@hotmail.com (Y. Ren), hjZhu@mail.kib.ac.cn (H.-j. Zhu).
[1] Co-corresponding author: Tel.: +86-871-5223242; fax: +86-871-5216179.

1387-3806/$ – see front matter © 2003 Elsevier B.V. All rights reserved.
doi:10.1016/S1387-3806(03)00308-7

In order to compare the gas-phase S_N2 at nitrogen with at carbon systematically, it is necessary to make a detail study for the fundamental non-identity S_N2 reactions at nitrogen (Eq. (2)).

$$Y^- + NH_2X \rightarrow NH_2Y + X^- \quad (Y, X = F, Cl, Br \text{ and } I) \tag{2}$$

It is clear from the very large number of calculations already carried out on S_N2 reactions that the computational data are very sensitive to the level of theory employed [16–20]. The G2 (+) theory introduced by Glukhovtsev et al. had been used successfully in theoretical studies of S_N2 reactions at carbon [12a–12c], nitrogen [9]. Hybrid Hartree–Fock density–function theory is of great interest for computational thermochemistry and thermochemical kinetics. Its low computational cost compared to ab initio methods makes it a very attractive alternative for many applications. Martin and coworkers [5] studied the gas-phase S_N2 reactions at carbon $Y^- + CH_3X \rightarrow CH_3Y + X^-$ (X, Y = F, Cl, Br) using a serious of high-level ab initio computational thermochemistry methods and eight density functional methods and concluded that the MPW1K functional appeared to put in the best performance on all DFT methods considered. Our previous study [21] also showed that MPW1K method with 6-31+G (d, p) could well reproduce the results of G2 (+) theory in describing the potential surface for the identity S_N2 reactions at neutral nitrogen (Eq. (3)) and reduce the mean unsigned errors over all energetics by a factor of 7 over MPW1PW and by a factor of 12.5 over B3LYP.

$$X^- + NH_2X \rightarrow NH_2X + X^- \quad (X = F, Cl, Br, I) \tag{3}$$

Now, we extend our hybrid DFT study to non-identity amino-transfer reactions (Eq. (2)). The present work represents the first computational study of this fundamental reaction for all of the halogens at the DFT level and will hopefully provide some useful information about the energy parameter. We also wish to apply the Marcus theory to the displacement S_N2 reactions at nitrogen. Meanwhile, we will discuss the nucleophilicity and leaving-group ability of halide anion in gas-phase S_N2 reactions at nitrogen.

2. Methods

All structures of reactants, ion–molecule complexes, transition states and products were completely optimized at the level of MPW1K/6-31+G (d, p) using Gaussian'98 programs [22]. All electron (AE) calculations were run for the fluorine- and chlorine-containing species, while Wadt and Hay [23] effective core potentials (MPW1K-ECP) were used for bromine- and iodine-containing species.

Stationary points on potential energy surfaces were characterized using analytical frequencies at the same level: all ground states had only real frequencies and all transition states had one and only one imaginary frequency. A scaling factor of 0.9515 [24] was used for zero-point vibration energy (ZPVE) corrections in the calculation of relative energies for the various species involved in Eq. (2). Charge distributions were obtained from the geometry calculated at the MPW1K/6-31+G (d, p), employing natural population analysis (NPA) [25–29].

Throughout this paper, bond lengths are in angstroms, and bond angles are in degrees. Relative energies correspond to enthalpy changes at 0 K [ΔH (0 K)] in kJ/mol.

3. Results and discussion

The gas-phase reaction energy profile for the concerted S_N2 reactions at nitrogen is described by an asymmetrical double-well curve for the non-identity reactions (Fig. 1). The reaction involves the initial formation of a reactant ion–molecule complex **1**. This complex must then overcome the central activation barrier to reach an asymmetrical transition structure **2**. The latter then breaks down to give the product ion–molecule complex **3**, which subsequently dissociates into the separate products. Analysis of the overall enthalpy changes indicates that the gas-phase non-identity S_N2 reaction at nitrogen is exothermic if the nucleophile is the lighter halide, which is same as the corresponding non-identity S_N2 reactions at carbon [12]. The forward reactions are defined as exothermic in the following discussion.

The key energetic quantities involved in reactions (Eq. (2)), depicted in Fig. 1, are labeled as follows: ΔH_{YX}^{comp} and ΔH_{XY}^{comp} are the complexation energies for the ion–molecule complexes **1** and **3**, respectively. $\Delta H_{YX}^{\neq}$ and $\Delta H_{XY}^{\neq}$ are the central activation barriers, and ΔH_{YX}^{b} and ΔH_{XY}^{b} are the overall activation barriers, for the corresponding forward and reverse reactions. ΔH is the central enthalpy difference between the product and reactant ion–molecule complexes **1** and **3**. ΔH^{ovr} is the overall enthalpy change for the forward reaction.

3.1. NH_2X structures (X = F, Cl, Br, I)

The calculated NH_2X geometries were found to be in reasonable agreement with available experimental data [30,31] and the G2 (+) results [10] (Table 1). Comparing with G2 (+) geometries, all of the DFT bond lengths are found to be slightly underestimated and the mean signed error (MSE) and mean unsigned error (MUE) are −0.021 and 0.021 Å, respectively. All of the calculated ∠X–N–H angles are a little bit overestimated with the MSE value −0.9° and MUE value 0.9°. NPA charge distributions (Table 2) show that the fluorine atom in NH_2F bears a negative charge, in contrast to the results for the other NH_2X molecules where the chlorine, bromine and iodine atoms are found to bear a positive charge. While charges on the hydrogen change little from NH_2F to NH_2I, the negative charge on nitrogen increases considerably from NH_2F to NH_2I.

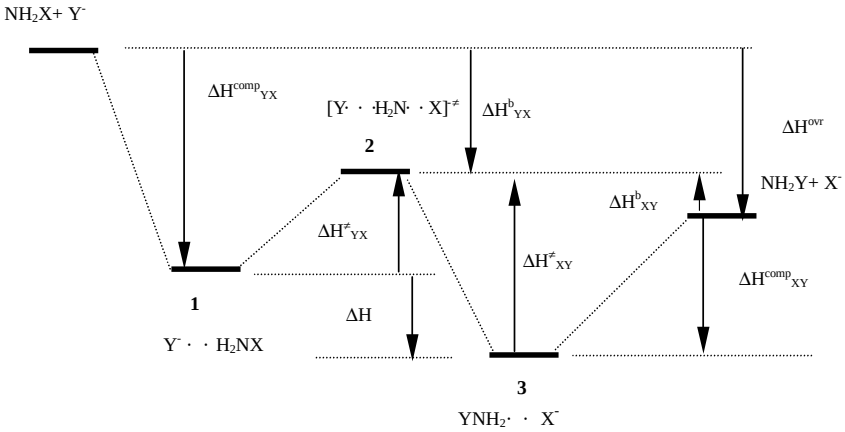

Fig. 1. Schematic potential energy surface for the non-identity gas-phase displacement reaction at nitrogen (Eq. (2)).

Table 1
Calculated geometries of NH_2X (X = F, Cl, Br, I)

Species	Level	r (N–X)	r (N–H)	X–N–H
NH_2F	MPW1K/6-31+G (d, p)	1.399	1.013	102.2
	MP2/6-31+G (d)[a]	1.446	1.024	100.6
	Expt.[b]	1.436	1.027	100.9
NH_2Cl	MPW1K/6-31+G (d, p)	1.728	1.010	105.6
	MP2/6-31+G (d)[a]	1.752	1.022	105.2
	Expt.[c]	1.748	1.017	103.7
NH_2Br	MPW1K/6-31+G (d, p)-ECP	1.885	1.010	105.1
	MP2/6-31+G (d)-ECP[a]	1.920	1.023	104.2
NH_2I	MPW1K/6-31+G (d, p)-ECP	2.057	1.010	106.1
	MP2/6-31+G (d)-ECP[a]	2.083	1.024	105.4

[a] From [9].
[b] From [30].
[c] From [31].

3.2. Ion–molecule complexes

Glukhovtsev et al. [9] pointed out that X^- can approach to NH_2X through three types to form three possible conformers for the ion–molecule complexes, in which the halide ion coordinates with just one hydrogen (type 1), with two hydrogen atoms (type 2), or with halogen atom of NH_2X molecule (type 3). The G2 (+) calculation indicated the preferred structures for all of $X^- \cdots H_2NX$ ion–molecule complexes are the type 1 with C_1 symmetry. Therefore, type 2 and type 3 are not considered here.

3.2.1. Geometries

Calculated geometries of the complexes are shown in Fig. 2. The geometries of the NH_2X (NH_2Y) moieties within the $Y^- \cdots H_2NX$ or $X^- \cdots H_2NY$ species differ only slightly from those in unperturbed NH_2X (NH_2Y). A slight elongation of the H–N and N–X (N–Y) lengths and an increase in angles ∠H–N–X (or ∠H–N–Y) relative to the values in isolated molecules NH_2X (NH_2Y) are characteristic features of the geometries of the ion–molecule complexes **1** and **3**. The extent of elongation of the H–N bond can be measured by the parameter %N–H proposed by Glukhovtsev et al. [9] (Eq. (4)), where r^{comp} (H–N) and r^{react} (H–N) are the H–N bond lengths in the ion–molecule complex **1** or **3** and in the reactant NH_2X or NH_2Y molecule, respectively.

$$\%\text{N–H} = 100 \times \frac{r^{comp}(\text{N–H}) - r^{react}(\text{N–H})}{r^{react}(\text{N–H})} \quad (4)$$

Table 2
NPA charge distributions for NH_2X (F, Cl, Br and I)

Species	q (N)	q (H)	q (NH_2)	q (X)
NH_2F	−0.466	0.379	0.29	−0.291
NH_2Cl	−0.899	0.416	−0.068	0.068
NH_2Br	−0.999	0.421	−0.157	0.157
NH_2I	−1.102	0.422	−0.258	0.258

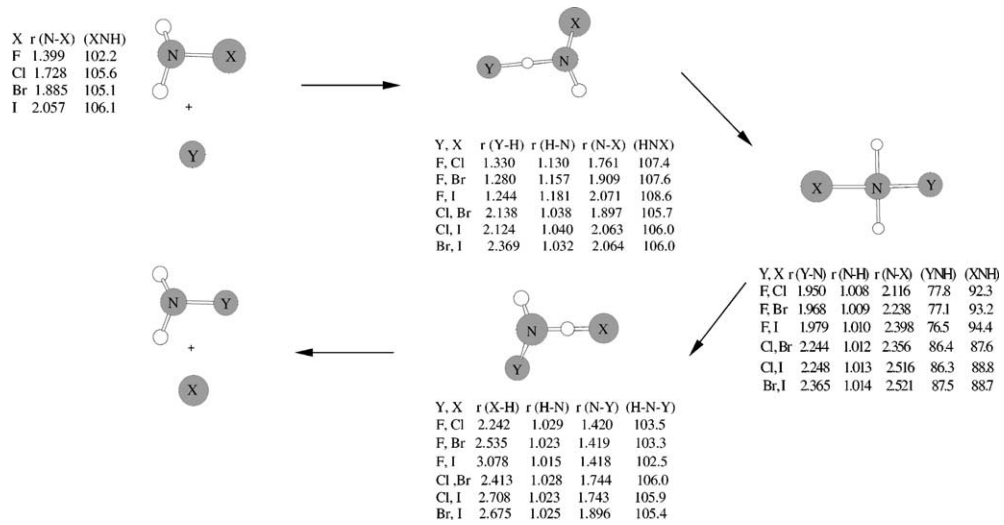

Fig. 2. Main geometries of the reactants, complexes and the transition structures in the reactions $Y^- + NH_2X \rightarrow NH_2Y + X^-$ (Y, X = F, Cl, Br, I) at the level of MPW1K/6-31+G (d, p).

There is a well-defined linear relationship between the complexation energies and %N–H (Fig. 3, $R^2 = 0.970$).

3.2.2. Complexation energies

The set of the MPW1K/6-31+G (d, p) complexation energies, ΔH_{YX}^{comp} and ΔH_{XY}^{comp}, for the complexes $Y^- \cdots H_2NX$ (Y, X = F, Cl, Br, I) are given in Table 3 with corresponding energy values for the $Y^- \cdots H_3CX$ (Y, X = F, Cl, Br, I) at the G2 (+) level.

The complexation energies for non-identity reactions $Y^- \cdots H_2NX$ are larger than the corresponding values in non-identity S_N2 at carbon, which are consistent with the N–H bond being an effective proton donor, leading to significant $Y^- \cdots HN$ or $NH \cdots X^-$ hydrogen bonding in the complexes $Y^- \cdots H_2NX$ and $YNH_2 \cdots X^-$. The set of complexation enthalpies also indicates that the complexation enthalpies depend primarily on the identity of nucleophile Y^-, and only to a small extent on the identity of NH_2X, and tend to decrease in the basicity order in the gas phase:

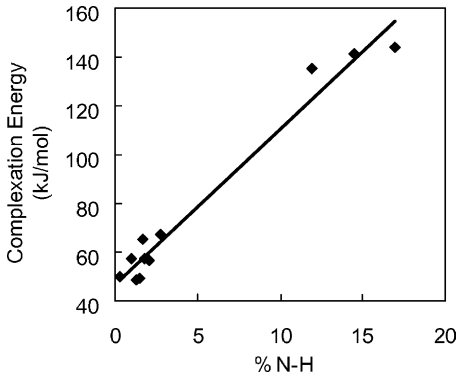

Fig. 3. Plot of MPW1K/6-31+G (d, p) complexation energies for S_N2 reactions $Y^- + NH_2X \rightarrow NH_2Y + X^-$ (Y, X = F, Cl, Br, I) vs. the extent of elongation of the N–H bond (see Eq. (4)). The values are listed in Table 3.

$F^- > Cl^- > Br^- > I^-$, which is analogous to those found for S_N2 reactions at carbon [12b] and oxygen [32]. Thus, the complexation energies for $Y = F^-$ range between 124.9 and 144.0 kJ/mol, those for $Y = Cl^-$ range between 65.3 and 67.5 kJ/mol, those for $Y = Br^-$ range between 56.8 and 57.9 kJ/mol, while those for $Y = I^-$ range between 47.9 and 49.8 kJ/mol.

For a given NH_2X, the complexation energies show a good linear correlation with electronegativities of the halogen Y^- ($R^2 \approx 0.946$ for Y = F, Cl, Br and I, respectively).

3.3. Transition state structure and barrier heights

MPW1K/6-31+G (d, p) geometries of transition structures $[Y \cdots H_2N \cdots X]^{-\neq}$ are shown in Fig. 2. Hybrid DFT values for the central barriers and overall barriers are listed in Table 4.

3.3.1. Geometries

The TS structures at the MPW1K/6-31+G (d, p) level of theory are found to have Cs symmetry for the non-identity reactions. The N–H bond lengths are similar in magnitude, increasing marginally from 1.008 to 1.141 Å, which is analogous to the corresponding reactions at carbon. The key parameters for describing the transition state are the distance between the halogen anion and the nitrogen atom. The main geometric feature in the transition structures is the elongation of the N–X and N–Y bonds relative to the ion–molecule complex. In a way similar to that proposed for Eq. (1) [2], we can readily define the geometrical looseness in the transition structures, $\%N–X^{\neq}$ and $\%N–Y^{\neq}$, and the composite transition structure looseness $\%L^{\neq}$:

$$\%N–X^{\neq} = 100 \times \frac{r^{\neq}(N–X) - r^{comp}(N–X)}{r^{comp}(N–X)} \quad (5)$$

Table 3
DFT complexation enthalpies (ΔH^{comp}) of the ion–molecule complexes, **1** and **3**

	F^-	Cl^-	Br^-	I^-
NH_2F	124.9 (7.9)[a], **114.0** (**5.0**)[b]	65.3 (1.7)	57.3 (1.0)	49.8 (1.8)
[12][c]	*56.5*	*39.3*	*34.6*	*30.7*
NH_2Cl	135.6 (11.9)	66.6 (2.5), **67.8** (**1.8**)	57.3 (0.3)	48.8 (1.3)
[12][b]	*64.4*	*44.0*	*39.0*	*34.4*
NH_2Br	141.6 (14.5)	67.5 (2.8)	57.9 (2.0), **58.4** (**1.5**)	49.1 (1.5)
[12][b]	*68.9*	*46.3*	*41.1*	*36.3*
NH_2I	144.0 (16.9)	66.5 (2.9)	56.8 (2.1)	47.9 (1.6), **50.0** (**1.3**)
[12][b]	*69.6*	*45.8*	*40.7*	*36.0*

[a] Values in parentheses are the extent of the elongation of the H–N bond.
[b] Values in bold are the G2 (+) complexation energies for reactions $X^- + NH_2X$ from [9].
[c] Values in italic are the G2 (+) complexation energies for reactions $Y^- + CH_3X$ from [12b].

$$\%N\text{–}Y^{\neq} = 100 \times \frac{r^{\neq}(N\text{–}Y) - r^{comp}(N\text{–}Y)}{r^{comp}(N\text{–}Y)} \quad (6)$$

$$\%L^{\neq} = \%N\text{–}X^{\neq} + \%N\text{–}Y^{\neq} \quad (7)$$

where $r^{\neq}$ (N–X) or $r^{\neq}$ (N–Y) and r^{comp} are the bond lengths in the transition structure **2** and the ion–molecule complex (**1** or **3**), respectively.

The geometrical asymmetry of the transition structure **2** is defined by

$$\%AS^{\neq} = \%N\text{–}Y^{\neq} - \%N\text{–}X^{\neq} \quad (8)$$

All of these measures of transition structure looseness and asymmetry are presented in Table 5 and their correlations with some of the other properties related to the reactions (Eq. (2)) are discussed below.

Table 5
Looseness and asymmetry index of the transition structures **2** $[Y\cdots H_2N\cdots X]^{-\neq}$ (Y, X = F, Cl, Br, I)

Y, X	$\%N\text{–}X^{\neq}$	$\%N\text{–}Y^{\neq}$	$\%L^{\neq}$	$\%AS^{\neq}$
F, Cl	20.1	37.3	57.4	17.1
F, Br	17.2	38.7	55.8	21.5
F, I	15.7	39.6	55.4	23.8
Cl, Br	24.2	28.7	53.0	4.5
Cl, I	21.9	28.9	50.9	7.1
Br, I	22.1	24.7	46.9	2.6

3.3.2. Barrier heights

For the non-identity reactions at nitrogen (Eq. (2)), the calculated central barriers at 0 K range from the 39.9 kJ/mol for the forward reaction $Br^- + NH_2I$ up to 87.4 kJ/mol for the reverse reaction $I^- + NH_2F$. According to the Marcus

Table 4
Energetics (kJ/mol) of the reactions $Y^- + NH_2X \rightarrow X^- + NH_2Y$ (Y, X = F, Cl, Br, I)

Y, X	$\Delta H^{\neq}_{YX}$	ΔH^{b}_{YX}	ΔH^{b}_{XY}	$\Delta H^{\neq}_{XY}$	ΔH	ΔH^{ovr}
F, F	78.9 (58.2)[a]	−46.0 (−55.8)				
Cl, Cl	60.9 (58.5)	−5.6 (−9.3)				
Br, Br	44.9 (44.7)	−13.0 (−13.7)				
I, I	33.6 (39.1)	−14.3 (−10.8)				
F, Cl	75.2 (**64.6**)[b]	−60.4 (**−60.5**)	20.8 (**20.8**)	86.1 (**75.5**)	−10.9	−81.3
	11.9 (***13.4***)[c]	*−52.5* (***−42.4***)	*75.0*	*114.3*	*−102.4*	*−127.5*
F, Br	71.9 (**54.75**)	−69.7 (**−69.1**)	29.3 (**29.9**)	86.6 (**69.45**)	−14.7	−99.0
	3.1 (***5.5***)	*−65.8* (***−50.1***)	*93.8*	*128.4*	*−125.3*	*−159.6*
F, I	74.5 (**50.0**)	−69.5 (**−70.9**)	37.6 (**36.2**)	87.4 (**62.9**)	−12.9	−107.1
	0.8 (***2.5***)	*−68.9* (***−48.5***)	*108.6*	*139.7*	*−138.9*	*−177.5*
Cl, Br	49.8 (**49.2**)	−17.6 (**−17.8**)	0.1 (**–0.1**)	57.3 (**56.7**)	−7.5	−17.7
	39.5 (***39.6***)	*−6.8* (***−5.9***)	*25.3*	*64.3*	*−24.8*	*−32.1*
Cl, I	46.2 (**43.3**)	−20.3 (**−22.0**)	5.5 (**3.8**)	54.3 (**51.4**)	−8.1	−25.8
	32.0 (***31.6***)	*−13.8* (***−12.1***)	*36.1*	*70.6*	*−38.6*	*−49.9*
Br, I	39.9 (**39.0**)	−16.9 (**−17.6**)	−8.8 (**−9.5**)	40.3 (**39.4**)	−0.4	−8.1
	38.4 (***38.2***)	*−2.3* (***−2.3***)	*15.6*	*51.9*	*−13.5*	*−17.9*

[a] Values in parentheses are energetics of the $X^- + NH_2X \rightarrow X^- + NH_2X$ reactions at G2 (+) level from [9].
[b] Values in bold are the calculated central barriers with Eq. (10) and overall barriers with Eq. (11).
[c] Values in italic are the energetics of the $Y^- + CH_3X \rightarrow X^- + CH_3Y$ reactions at G2 (+) level from [12b], in which the bold are calculated with Eqs. (10) and (11).

theory [13–15], in an exothermic reaction, a thermodynamic driving force will lower the transition state energy whereas endothermic driving force will induce higher activation energy. So, the forward central barrier heights $\Delta H^{\neq}_{YX}$ should be lower than the intrinsic central barrier $\Delta H^{\neq}_{0\,YX}$ and the reverse central barrier heights $\Delta H^{\neq}_{XY}$ should be higher than the intrinsic central barrier $\Delta H^{\neq}_{0\,YX}$. $\Delta H^{\neq}_{0\,YX}$ is estimated using the additivity postulate:

$$\Delta H^{\neq}_{0\,YX} = 0.5[\Delta H^{\neq}_{YY} + \Delta H^{\neq}_{XX}] \quad (9)$$

The DFT central barriers in Table 4 show that all of the reverse reactions are in agreement with Marcus theory. As for the forward reactions, Marcus theory can successfully apply to the reactions $Y^- + NH_2X$ (Y, X = Cl, Br, I), but breaks down for the reactions $F^- + NH_2X$ (X = Cl, Br, I), which may be attributed to the overestimation of central barriers for the reactions $F^- + NH_2X$ (X = F, Cl, Br, I) at the level of MPW1K/6-31+G (d, p). In our recent papers, the MPW1K/6-31+G (d, p) method is found to predict too short $F^- \cdots H$ distance and too high interaction energy, which will induce the overestimation of complexation energies for the $F^- \cdots H_2NF$ [21] and $F^- \cdots HOF$ [32] systems and the central barriers for the $F^- + H_2NF$ and $F^- + HOF$ reactions. These phenomena will still exist in the non-identity reactions $F^- + NH_2X$ (X = Cl, Br, I).

The forward overall barriers ΔH^{b}_{YX} for $Y^- + NH_2X$ are all negative, analogous to the corresponding values for non-identity substitution reactions at carbon [12]. In reverse direction, only the overall barrier for the reaction $I^- + NH_2Br$ is negative, whereas all positive for the corresponding reactions at carbon. All of the forward overall barrier ΔH^{b}_{YX} for $Y^- + NH_2X$ systems are lower than the corresponding values for carbon, which suggests that nucleophilic substitution reactions at nitrogen are more energetically facile than at carbon.

3.3.3. Charge distributions

The charge distributions of the transition states in Table 6 reveal a substantial positive charge on the NH_2 moiety for the $[F \cdots H_2N \cdots X]^{-\neq}$ (X = F, Cl, Br, I). This presumably reflects a significant contribution of the triple-ion valence bond configuration, $F^-(NH_2^+)X^-$ (X = F, Cl, Br and I). This mixing of the triple-ion configuration may be responsible for the stabilization of the transition state, leading to the lower ΔH^{b}_{YX} values than the other transition structures $[Y \cdots H_2N \cdots X]^{-\neq}$ (Y, X = Cl, Br, I), in which the NPA charges on the NH_2 moiety are almost zero.

The asymmetry of the charges distributions in the transition state can be described by the difference $\Delta q(X - Y) = q(X) - q(Y)$. Correlation involving $\Delta q(X - Y)$ values are discussed in the next section.

3.4. Correlations of barrier heights

There have been considerable discussions in the literature as to what factors might influence the barrier heights in gas-phase S_N2 reaction [9,12a,12b,32]. In this section, we will briefly discuss our computational data for the non-identity S_N2 reactions at nitrogen. We will seek the relationship between the barrier heights and some properties related to reactions and check whether the non-identity substitution reactions at nitrogen show similar pattern of behavior to substitution at carbon.

3.4.1. Rate–equilibrium relationship

Marcus theory has been successfully applied to the interpretation of gas-phase S_N2 reactions at carbon and oxygen. It will be interesting to test the reliability of the Marcus theory for the S_N2 reactions at nitrogen. The Marcus equation

$$\Delta H^{\neq}_{YX} = \Delta H^{\neq}_{0\,YX} + 0.5\,\Delta H + \left[\frac{(\Delta H)^2}{16\,\Delta H^{\neq}_{0\,YX}}\right] \quad (10)$$

relates the intrinsic barrier heights of a non-identity substitution reaction to the corresponding intrinsic barrier height in the absence of a thermodynamic driving force and the central enthalpy difference between product and reactant ion–molecule complexes **3** and **1**. We can see from Table 4 that the DFT central barriers for the reactions involving the fluorine are significantly higher than the Marcus central barriers deduced by Eq. (10) because the hybrid DFT method overestimate the central barrier for the $F^- + NH_2X$ (X = F–I) reactions. For the other reactions $Y^- + NH_2X$ (Y, X = Cl, Br, I), the DFT central barrier heights are reproduced by

Table 6
NPA charge distributions for the transition states $[Y \cdots H_2N \cdots X]^{-\neq}$

Y, X	q (Y)	q (X)	q (N)	q (H)	q (NH_2)	Δq (X − Y)
F, F	−0.674	−0.674	−0.448	0.398	0.349	0
Cl, Cl	−0.561	−0.561	−0.711	0.417	0.122	0
Br, Br	−0.512	−0.512	−0.808	0.416	0.025	0
I, I	−0.450	−0.450	−0.922	0.411	−0.100	0
F, Cl	−0.729	−0.488	−0.619	0.418	0.217	0.240
F, Br	−0.728	−0.439	−0.675	0.421	0.167	0.289
F, I	−0.724	−0.389	−0.730	0.422	0.113	0.334
Cl, Br	−0.557	−0.518	−0.758	0.417	0.076	0.039
Cl, I	−0.547	−0.474	−0.808	0.414	0.021	0.072
Br, I	−0.500	−0.467	−0.861	0.414	−0.034	0.032

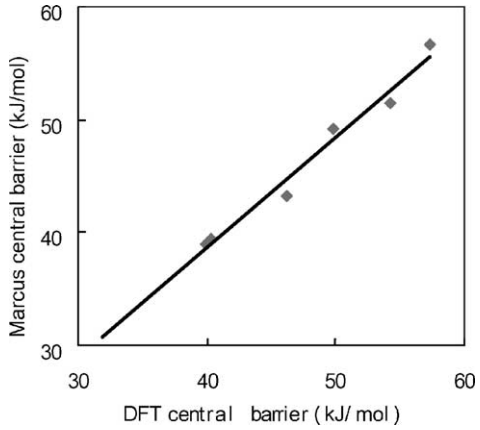

Fig. 4. Plot of central barriers from Eq. (10) vs. the same quantity obtained directly from the hybrid DFT method MPW1K/6-31+G (d, p) (Y, X = Cl, Br, I). The values are listed in Table 4.

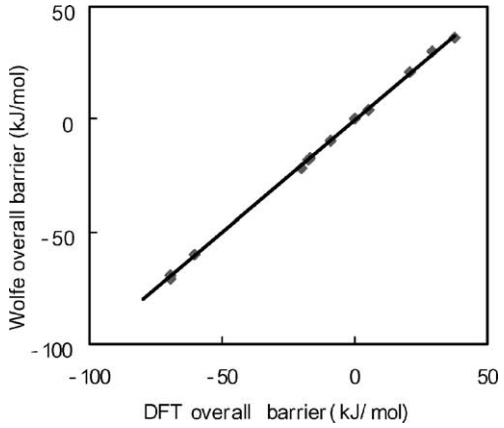

Fig. 5. Plot of overall barriers from Eq. (11) vs. the same quantity obtained directly from MPW1K/6-31+G (d, p) (Y ≠ X; Y, X = F, Cl, Br and I). The values are listed in Table 4.

Marcus theory within a few kJ/mol (the largest difference and MSE being 2.9 and −1.5 kJ/mol, respectively). A plot of Marcus central barriers by Eq. (10) versus the corresponding DFT data for the reactions $Y^- + NH_2X$ (Y, X = Cl, Br, I) gives a good linear correlation (see Fig. 4, $R^2 = 0.976$).

In order to apply the Marcus equation to the overall barriers, rather than the central barrier, Wolfe et al. [33] proposed the following modifications:

$$\Delta H^{b}_{YX} = \Delta H^{b}_{0\,YX} + 0.5\,\Delta H_{ovr} + \left[\frac{(\Delta H^{ovr})^2}{16\,\Delta H^{\neq}_{0\,YX}}\right] \quad (11)$$

$$\Delta H^{b}_{0\,YX} = 0.5[\Delta H^{b}_{YY} + \Delta H^{b}_{XX}] \quad (12)$$

The Eqs. (11) and (12) permit the predictions of the experimentally more accessible quantity from data of the corresponding identity reactions. The data in Table 4 illustrate the applicability of Wolfe equation to all of non-identity S_N2 reactions at nitrogen, the largest difference and MSE just being 1.7 and −0.6 kJ/mol, respectively. There is a better correlation between the overall barriers obtained by Wolfe equation versus the corresponding DFT barriers (see Fig. 5, $R^2 = 1.000$) for Eq. (2) than corresponding correlation existed in Eq. (1), that may be attributed to the smaller exothermicity for Eq. (2) [12b].

3.4.2. Correlation of central barriers and overall barriers

In the non-identity reactions at carbon (Eq. (1)), a good correlation was found between the central barrier ($\Delta H^{\neq}_{YX}$), overall barrier (ΔH^{b}_{XY}) with the overall enthalpy change (ΔH^{ovr}) for the forward reactions [12b]. For the non-identity S_N2 reactions at nitrogen (Eq. (2)), there are also similar good correlations ($R^2 = 0.929$ and 0.999, respectively). Furthermore, as observed in Eq. (1), we find a reasonable correlation between the central barriers and the composite transition structure looseness, $\%L^{\neq}$ ($R^2 = 0.867$). Central barriers are also found to correlate with the geometrical asymmetry of the transition state, $\%AS^{\neq}$, and the charge distribution asymmetry, Δq (X−Y) ($R^2 = 0.901$ and 0.906, respectively), which is similar to the previous results in the non-identity methyl-transfer reactions (Eq. (1)) [12b].

For the $Y^- + CH_3X$ reactions (Eq. (1)), there is good correlation between the geometrical asymmetry of the TS, $\%AS^{\neq}$, and the charge asymmetry, Δq (X−Y), which means the early TS structures in a geometrical sense are also early in a charge sense. This pattern is reproduced in the non-identity S_N2 reactions at nitrogen ($R^2 = 0.994$).

There is a good correlation between central barrier heights and overall barrier heights for forward direction ($R^2 = 0.994$) in the G2 (+) study on the non-identity S_N2 reactions at carbon [12b]. This correlation also reasonably existed in the present DFT results on the non-identity S_N2 reactions at nitrogen ($R^2 = 0.923$), but the slope is negative (Fig. 6).

All of above correlations existed in the non-identity S_N2 at nitrogen and the comparison with the results for the $Y^- + CH_3X$ (Y, X = F, Cl, Br and I) reactions at the G2 (+) level were summarized in Table 7.

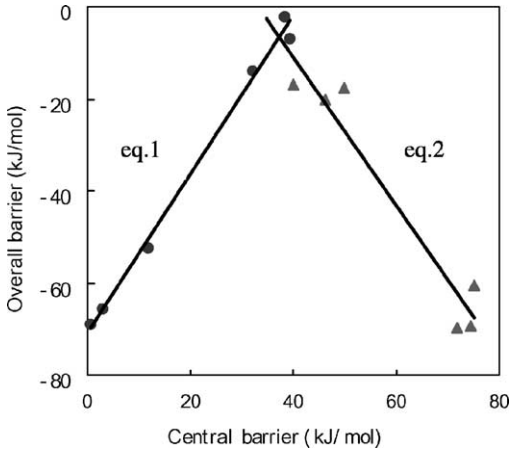

Fig. 6. Plot of central barrier vs. the overall barriers. The values involving non-identity S_N2 reactions at nitrogen (Eq. (2)) at the level of MPW1K/6-31+G (d, p) are listed in Table 4. The G2 (+) values for non-identity S_N2 reactions at carbon (Eq. (1)) are from [12b].

Table 7
Linear correlations of various characteristics of the reactions $Y^- + NH_2X \rightarrow X^- + NH_2Y$ (Y, X = F, Cl, Br, I)

Entry	Parameter 1	Parameter 2	R^2[a]
1[a]	$\Delta H^{\neq}_{YX}$	ΔH^{ovr}	0.929 (0.991)[b]
2	$\Delta H^{\neq}_{YX}$	$\Delta H^{\neq}_{YX}$ (Marcus, Eq. (10))	0.976* (0.999)
3	$\Delta H^{\neq}_{YX}$	Δq (X − Y)	0.906 (0.912)
4	$\Delta H^{\neq}_{YX}$	$\%L^{\neq}$	0.867 (0.821)
5	$\Delta H^{\neq}_{YX}$	$\%AS^{\neq}$	0.901 (0.922)
6	ΔH^{b}_{YX}	ΔH^{b}_{YX} (Wolfe, Eq. (11))	1.000 (0.994)
7	ΔH^{b}_{YX}	ΔH^{ovr}	0.999 (0.995)
8	Δq (X − Y)	$\%AS^{\neq}$	0.994 (0.995)
9	$\Delta H^{\neq}_{XY}$	ΔH^{b}_{YX}	0.923 (0.994)
10	ΔH^{ovr}	ΔH	0.845* (1.000)

[a] Marked values are for Y, X = Cl, Br, I; unmarked values are for Y, X = F, Cl, Br, I.
[b] Values in parentheses are the corresponding correlations at carbon from [12b].

3.5. Nucleophilicity and leaving-group ability of halides in gas-phase S_N2 reactions at nitrogen

The orders of nucleophilicity and the leaving-group ability are essential that describe for S_N2 reactions and will strongly affects the rate of the S_N2 reactions. Many properties have an influence on nucleophilicity, such as the medium of S_N2 reactions, the strength of its bond with central atom, and the electronegativity of the attacking atom. In the aliphatic S_N2 reactions, nucleophilicity of nucleophile in the solvent may be different from in the gas phase because of the solvation energy. The observed [34] and predicted [35,36] sequences of nucleophilcity in the gas-phase S_N2 reaction at carbon follow the order: $F^- > Cl^- > Br^- > I^-$, which will be reverse in the dipolar solvent, such as water and the alcohol. Here, we will discuss the nucleophilicity and leaving-group ability of different halides in the gas-phase S_N2 reactions at nitrogen (Eqs. (1) and (2)) using our DFT energetics in Table 4.

3.5.1. Thermodynamic study

As shown in previous work [34], the exothermicity of the reactions of nucleophile with a single substrate reflects the thermodynamic affinity of the nucleophile. Following this idea, the exothermicity trend, in this work, is given by the sequences of the overall enthalpy change ΔH^{ovr} for the forward reaction as a function of nucleophile X^-. The more negative of ΔH^{ovr}, the stronger of the exothermicity of the reaction.

No matter Y^- react any substrate, NH_2F, NH_2Cl, NH_2Br or NH_2I, the exothermicity falls in following order (see Table 4):

$$F^- > Cl^- > Br^- > I^-$$

These sequences are in agreement with the available experimental results [11]. This exothermicity can be clearly related to the nucleophilicity of X^-, which follows the same trend.

If we fix the nucleophile Y^- and change the substrate NH_2X going from X = F to I, the exothermicity of the reactions increase in the same direction. This is certainly related to the leaving-group ability, following in the order: F < Cl < Br < I.

3.5.2. Kinetic study

High-level computational study of Glukhovtsev et al. [9] for identifying S_N2 reactions at nitrogen (Eq. (3)) suggests that the more negative overall barrier heights, the more facile for the S_N2 reactions. The overall barriers for reactions $Y^- + NH_2X$ (Y = F, Cl, Br, I; X = F), as indicated in Table 4, shows that the sequence given by ΔH^{b}_{YX} and ΔH^{b}_{XY} follows the order:

$$F^- < Cl^- < Br^- < I^-$$

With other three substrates NH_2Cl, NH_2Br and NH_2I the same orders are obtained (see Table 4). These results are in good agreement with the exothermicity of reaction given in Eq. (2), showing the correlation between overall barriers and the overall reaction enthalpy, i.e., when the overall barriers decrease the exothermicity of the reactions increases. What is more, for a given nucleophile Y^-, the calculated overall barriers decrease when going from X = F to I, which relates the leaving-group ability increasing from F to I. In summary, the investigations of kinetic and thermodynamic for Eq. (2) lead to the same conclusions.

3.5.3. Basicity and nucleophilicity of X^-

In the experimental study on the gas-phase S_N2 reactions at nitrogen [11], the reaction efficiency is found to increase systematically with increasing basicity of reactant anion. Previous experiments [37] and calculations [32,38] have indicated that the gas-phase acidity of HX (X = F–I) increase in the order: HF < HCl < HBr < HI, which implies the basicity of X^- will decrease in the following order: $F^- > Cl^- > Br^- > I^-$. This order is consistent with nucleophilicity of X^-.

4. Conclusions

The exchange reactions at the saturated nitrogen atom $Y^- + NH_2X \rightarrow NH_2Y + X^-$ (Y, X = F, Cl, Br, I) were investigated at the MPW1K/6-31+G (d, p) level of theory, leading to the following conclusions:

(1) The energy profile for the gas-phase non-identity S_N2 at nitrogen is described by an asymmetric double-well curve. The following pathway for the model reactions is established:

$$Y^- + NH_2X \rightarrow Y^- \cdots H_2NX \rightarrow [Y \cdots H_2N \cdots X]^{-\neq} \rightarrow YNH_2 \cdots X^- \rightarrow NH_2Y + X^-$$

(2) In asymmetrical displacement reactions at nitrogen, the enthalpies of reactions are exothermic only when the nucleophile is the lighter halide, in agreement with those in non-identity substitution reactions at carbon.
(3) The ion–molecule complexation energies at 0 K increase from 48.8 kJ/mol for $I^- \cdots H_2NCl$ to 144.0 kJ/mol for $F^- \cdots H_2NI$. These values are found to be larger than those found for the corresponding carbon complexes $Y^- \cdots H_3CX$ and correlate well with the elongation parameter %N–H and the electronegativities of the nucleophile.
(4) The forward central barrier heights $\Delta H^{\neq}_{YX}$ (Y, X = Cl, Br, I) vary from 39.9 kJ/mol for the reaction $Br^- + NH_2I$ to 49.8 kJ/mol for the reaction $Cl^- + NH_2Br$ and the reverse central barrier heights $\Delta H^{\neq}_{YX}$ (Y, X = Cl, Br, I) vary from 40.3 kJ/mol for the reaction $I^- + NH_2Br$ to 57.3 kJ/mol for the reaction $Br^- + NH_2Cl$. The $\Delta H^{\neq}_{YX}$ are lower than the intrinsic central barrier $\Delta H^{\neq}_{0\,YX}$ and the lowering is attributed to the effect of forward reaction exothermicity which ranges from −25.8 kJ/mol for $Cl^- + NH_2I$ to −8.1 kJ/mol for $Br^- + NH_2I$.
(5) All of the forward overall barriers ΔH^{b}_{YX} for the reactions $Y^- + NH_2X \rightarrow NH_2Y + X^-$ (Y, X = F, Cl, Br, I) are negative and the corresponding barriers in the methyl exchange reactions $Y^- + CH_3X \rightarrow CH_3Y + X^-$ (varying from −69.7 kJ/mol for $F^- + NH_2Br$ to –16.9 kJ/mol for $Br^- + NH_2I$), which suggest that S_N2 reactions at nitrogen may be more facile than at carbon.
(6) The set of non-identity reactions $Y^- + NH_2X$ (Y, X = Cl, Br, I) obeys the Marcus equation. The central barriers estimated by Marcus equation (Eq. (10)) are close to the directly calculated central barrier and a plot of the two data sets gives a good correlation ($R^2 = 0.976$). A modified Marcus equation used to estimate the overall barriers for reactions $Y^- + NH_2X$ (Y, X = F, Cl, Br, I) is found to be more reliable ($R^2 = 1.000$).
(7) Forward central barriers, $\Delta H^{\neq}_{YX}$, exhibit reasonable linear relationship with the composite geometric looseness $\%L^{\neq}$, the geometrical asymmetry of the TS, $\%AS^{\neq}$, the charge distribution asymmetry, Δq (X − Y), and the overall enthalpy changes, ΔH^{ovr}.
(8) Combining the DFT results of kinetic and thermodynamic investigations, we predict that the nucleophilicity for halide anions in the reactions (Eq. (2)) follows the order: $F^- > Cl^- > Br^- > I^-$, and the leaving-group ability is reverse: F < Cl < Br < I, which is the same as S_N2 reactions at carbon.

Acknowledgements

The authors in Sichuan University are thankful for the support from the Barbara and Kort Sino-Israel Post-Doctoral Fellowship Program, the Scientific Research Foundation for the Returned Chinese Scholars of State Education Ministry. H.J. Zhu acknowledges the support of “Bairenjihua” Fund from CAS and the Fund (NSFC#20242012).

References

[1] C.K. Ingold, Structure and Mechanism in Organic Chemistry, 2nd ed., Cornell University Press, Ithaca, 1969.
[2] S.S. Shaik, H.B. Schlegel, S. Wolfe, Theoretical Aspects of Physical Organic Chemistry, The S_N2 Mechanism, Wiley, New York, 1992.
[3] J.K. Laerdahl, E. Uggerud, Int. J. Mass. Spectrom. 214 (2002) 277 (and references cited therein).
[4] L. Sun, K. Song, W.L. Hase, Science 296 (2002) 875.
[5] S. Parthiban, G. de Oliveira, J.M.L. Martin, J. Phys. Chem. A 105 (2001) 895.
[6] J. Gao, J. Am. Chem. Soc. 113 (1991) 7769.
[7] P. Beak, J. Li, J. Am. Chem. Soc. 113 (1991) 2796.
[8] M. Bühl, H.F. Schaefer III, J. Am. Chem. Soc. 115 (1993) 9143.
[9] M.N. Glukhovtsev, A. Pross, L. Radom, J. Am. Chem. Soc. 117 (1995) 9012.
[10] Y. Ren, H. Basch, S. Hoz, J. Org. Chem. 67 (2002) 5891.
[11] R. Gareyev, S. Kato, V.M. Bierbaum, J. Am. Soc. Mass Spectrom. 12 (2001) 139.
[12] (a) M.N. Glukhovtsev, A. Pross, L. Radom, J. Am. Chem. Soc. 117 (1995) 2024;
(b) M.N. Glukhovtsev, A. Pross, L. Radom, J. Am. Chem. Soc. 118 (1996) 6273;
(c) M.N. Glukhovtsev, A. Pross, H.B. Schlegel, R.D. Bach, L. Radom, J. Am. Chem. Soc. 118 (1996) 11258.
[13] R.A. Marcus, Annu. Rev. Phys. Chem. 15 (1964) 155.
[14] R.A. Marcus, J. Phys. Chem. 72 (1968) 891.
[15] W.J. Albery, Annu. Rev. Phys. Chem. 31 (1980) 227.
[16] Y.J. Cho, L.S.R. Vande, L. Zhu, W.L. Hase, J. Chem. Phys. 96 (1992) 8275.
[17] Z. Shi, R.J. Boyd, J. Am. Chem. Soc. 113 (1991) 1072.
[18] S.S. Shaik, A. Ioffe, A.C. Reddy, A. Pross, J. Am. Chem. Soc. 116 (1994) 262.
[19] W.-P. Hu, D.G. Truhlar, J. Phys. Chem. 98 (1994) 1049.
[20] B.D. Wladkowski, J.I. Brauman, J. Phys. Chem. 97 (1993) 13158.
[21] Y. Ren, J.L. Wolk, S. Hoz, Int. J. Mass Spectrum. 221 (2002) 59.
[22] M.J. Frisch, G.W. Trucks, H.B. Schlegel, G.E. Scuseria, M.A. Robb, J.R. Cheeseman, V.G. Zakrzewski, J.A. Montgomery, R.E. Stratmann Jr., J.C. Burant, S. Dapprich, J.M. Millam, A.D. Daniels, K.N. Kudin, M.C. Strain, O. Farkas, J. Tomasi, V. Barone, M. Cossi, R. Cammi, B. Mennucci, C. Pomelli, C. Adamo, S. Clifford, J. Ochterski, G.A. Petersson, P.Y. Ayala, Q. Cui, K. Morokuma, D.K. Malick, A.D. Rabuck, K. Raghavachari, J.B. Foresman, J. Cioslowski, J.V. Ortiz, B.B. Stefanov, G. Liu, A. Liashenko, P. Piskorz, I. Komaromi, R. Gomperts, R.L. Martin, D.J. Fox, T. Keith, M.A. Al-Laham, C.Y. Peng, A. Nanayakkara, C. Gonzalez, M. Challacombe, P.M.W. Gill, B. Johnson, W. Chen, M.W. Wong, J.L. Andres, C. Gonzalez, M. Head-Gordon, E.S. Replogle, J.A. Pople, Gaussian’98, revision A.7, Gaussian Inc., Pittsburgh, PA, 1998.
[23] W.R. Wadt, P.J. Hay, J. Chem. Phys. 82 (1985) 284.
[24] B.J. Lynch, D.G. Truhlar, J. Phys. Chem. A 105 (2001) 2936.
[25] A.E. Reed, R.B. Weinstock, F. Weinhold, J. Chem. Phys. 83 (1985) 735.
[26] J.P. Foster, F. Weinhold, J. Am. Chem. Soc. 102 (1980) 7211.
[27] F. Weinhold, J.E. Carpenter, The Structure of Small Molecular and Ions, Plenum Press, New York, 1988, p. 227.
[28] A.E. Reed, F. Weinhold, J. Chem. Phys. 78 (1983) 4066.
[29] A.E. Reed, L.A. Curtiss, F. Weinhold, Chem. Rev. 88 (1988) 899.
[30] D. Christen, R. Minkwitz, R. Nass, J. Am. Chem. Soc. 109 (1987) 7020.

[31] M.D. Harmony, V.W. Laurie, R.L. Kuczkowski, R.H. Schwendeman, D.A. Ramsay, F.J. Lovas, W.J. Lafferty, A.G. Maki, J. Phys. Chem. Ref. Data. 8 (1979) 619.
[32] Y. Ren, J.L. Wolk, S. Hoz, Int. J. Mass. Spectrum. 225 (2002) 167.
[33] S. Wolfe, D.J. Mitchell, H.B. Schlegel, J. Am. Chem. Soc. 103 (1981) 76942.
[34] W.N. Olmstead, J.I. Brauman, J. Am. Chem. Soc. 99 (1977) 4219.
[35] S.S. Shaik, P.C. Hiberty, Adv. Quantum Chem. 26 (1995) 99.
[36] B. Safi, K. Choho, P. Geerlings, J. Phys. Chem. A 105 (2001) 591.
[37] NIST Standard Reference Database Number 69, July 2001, Release (http://webbook.nist.gov/chemistry).
[38] M.N. Glukhovtsev, A. Pross, L. Radom, J. Phys. Chem. 100 (1996) 3498.